

**Structural Changes Associated with Interactions Between Starch and Particles of TiO<sub>2</sub> or ZnSe**

Paul Bernazzani\*, Assistant Professor, Lamar University, [paul.bernazzani@lamar.edu](mailto:paul.bernazzani@lamar.edu)

Hari Krishna Reddy Pandi, Student, Lamar University, [pkrishna\\_27@yahoo.co.in](mailto:pkrishna_27@yahoo.co.in)

Vamshi Krishna Peyyavula, Student, Lamar University, [vams\\_peyyavula@yahoo.com](mailto:vams_peyyavula@yahoo.com)

**Abstract**

The effects of modifying the structure of the starch chain on the kinetics of enzymatic cleavage are presented. The structural modifications involved interactions between the biopolymer chains and two types of transition metal particles: ZnSe, and TiO<sub>2</sub>. The structural changes were followed using Raman spectroscopy and differential scanning calorimetry (DSC) while the enzymatic activity was determined using the starch-iodine complexation method. Results show that interactions with ZnSe increase the rate of digestion while interactions with TiO<sub>2</sub> significantly slow down the reaction. Structural analysis suggests that strain variations in the backbone are the driving forces behind the experimental observations.

Keywords: Starch, interactions, thermal analysis, kinetics

**Introduction**

Starch is a polymer of  $\alpha$ -D-glucose. It consists of two main components: a linear compound called amylose and a branched compound called amylopectin. Amylose is a linear isotactic polymer that typically consists of up to 3000 monomer units of glucose molecules interconnected by  $\alpha$ -1, 4 glycosidic bonds with virtually no 1,6 links [1-3]. Amylose generally tends to form a relatively stiff parallel left handed single helix or a stiffer left-handed double helix. The oxygen atoms in positions 2 and 6 of the glucose monomer lie on the outside surface of the helix, with the ring oxygen pointing inward. Under some conditions, perfectly aligned chains may form double stranded crystallites that are resistant to amylases [4]. The second and most abundant component of starch, amylopectin, consists of a more highly branched polycarbohydrate with  $\alpha$  – 1, 4 bonds that serve as the backbone and  $\alpha$  – 1, 6 branching points which occur approximately every 20-25 glucose units [2, 5].

The structurally important helices formed by amylose may assemble into crystalline structures called type V [6, 7]. This helix is composed of 6 glucose residues per turn and has been found to have a pitch between 0.791 and 0.817 nm [8, 9]. While it is formed easily by the inclusion of small molecules such as lipids into the helix cavity, the size of this cavity may vary and has been reported to be between 1.5 and 2.9 nm depending on the method and the molecular weight of the sample [10].

Many types of enzymes hydrolyze the  $\alpha$  – 1,4 glycosidic bonds in starch but the most common enzyme is called  $\alpha$ -amylase [11], and was used in this study. Starches with high amylose content generally have low digestion rates but Rao [12] found that rice varieties with high amylose content had faster digestion rates compared to rice varieties with low amylose content. Crystallinity also affects the enzyme hydrolysis with B-type crystals being less susceptible to enzyme attack than A-type [13, 14]. This emphasizes not only the complexity of factors influencing digestion properties but also the sensitivity of the kinetics of digestion to the starch chain morphology [15].

In the enzymatic biodegradation of starch, the enzyme first diffuses and binds to the solid substrate, cleaves the glycosidic bonds and unbinds [16]. The  $\alpha$ -amylase enzymatic hydrolysis is carried out by a side-by-side digestion mechanism: the amylase binds the substrate from the

side, that is, it binds the starch molecules in a direction parallel to the strands [14]. The reaction rate is mainly controlled by the structure of the substrate as it affects the enzyme diffusion, binding, and bond cleavage. Thus, the kinetics of digestion offers a good indication that structural changes occur in starch molecules. These changes are important contributors to the possible applications of starch polymers.

Apart from its obvious use as a food source and as an enhancer of the viscosity and texture of food products starch has a wide range of applications [17]. It is used as adhesives, stabilizers, coatings, binders, and molecular sieve, an encapsulating agent for the pesticides, as well as, in the pharmaceutical industry for coating, dusting tablets, as well as, a matrix for controlled release drugs [17-19].

Starch chain structure is the most important factor in any application [20]. An understanding and fine control of the structure is necessary for the development of a greater range of applications, possibly including building materials.

This paper presents the effects on the structure of starch of the presence of two types of transition metal particles: ZnSe, TiO<sub>2</sub> (rutile and anatase). Our hypothesis is that optimizing interactions with water insoluble particles can finely control the structure of starch. Hence, the particles will interact with starch, leading to changes in the structure of the biopolymer chains such that modifications in enzyme binding occur, leading to a decrease in enzymatic biodegradation. The choice for these types of particles is based on the observation that, in polystyrene thin films, surface interactions with TiO<sub>2</sub> decrease the glass transition temperature (T<sub>g</sub>) while surface interactions with ZnSe were found to increase T<sub>g</sub> [21].

Different mixtures of amylose and particles will be investigated. These mixtures will involve changes in crystalline structure and amount of the metal particles. Differential scanning calorimetry (DSC) and Raman spectroscopy will be used to determine the extent and nature of interactions on the starch chains, while enzymatic biodegradation studies will give a quantitative measure of the effect of the interactions.

## **Experimental**

### *Materials*

Soluble starch powder was obtained from Mallinckrodt Baker Inc. (Paris, Kentucky, USA) and was used without further purification. Type II A  $\alpha$ -amylase, extracted from *Bacillus Subtilis* with a DMA of 2 and a specific activity of 839 units/mg, was purchased from Sigma-Aldrich (Milwaukee, WI, USA) and kept refrigerated. Resublimed iodine crystals, were purchased from MCB Chemicals. Potassium iodide crystals (P-410) were purchased from Fisher Scientific (NJ, USA). Sodium hydroxide pellets were purchased from Fox Scientific, Inc (Alvarado, TX, USA). Sodium phosphate dibasic anhydrous powder and sodium phosphate monobasic were obtained from Mallinckrodt Baker Inc. (Paris, Kentucky, USA). TiO<sub>2</sub> and ZnSe particles were purchased from Sigma-Aldrich (Milwaukee, WI, USA),

### *Sample solutions*

Starch (0.5 g) was placed in a beaker and 5.0 mL of distilled water were added. Sodium hydroxide (1.0 mL, 0.1 M) was added and the mixture was heated at 50 °C with continuous stirring for 15 minutes until a clear solution was obtained. To this clear solution, 5.0 mL of a phosphate buffer solution (pH 7.4, 0.1 M) were added and stirred. To this solution, 4.0 mL of an iodine solution (0.001 M) were added until a blue colored solution was achieved.

A stock solution of  $\alpha$ -amylase was prepared by dissolution of 2.0 mg of  $\alpha$ -amylase in 5.6 mL of a 7.4 pH phosphate buffer solution (0.1 M) and stirred well to form a homogeneous solution. The

solution was refrigerated at -20°C when not in use. To the colored starch solution, 0.5 mL of the  $\alpha$ -amylase solution was added immediately before UV-Visible spectra were recorded.

#### *Digestion Kinetics by UV-Visible Spectrophotometer*

A Cary 50-Bio UV-Visible spectrophotometer was used to determine the relative amount of amylose-iodine complex formed, which is related to enzymatic degradation. A scan rate of 2400 nm/min was used and the scan range was 200-800 nm. Maximum absorbance was observed at 575 nm. Although TiO<sub>2</sub> absorbs slightly in this region, the small amount used could not be detected. Therefore no supplementary baseline corrections were performed. Scans were recorded every 60 seconds.

The digestion kinetics were evaluated by fitting the change in absorbance as a function of time to equation 1 using a Levenberg-Marquart fitting algorithm available in a software package (PSI Plot). Values of  $\tau$  and  $\beta$  are obtained from this fitting. The initial values for these parameters were kept at 10 and 1 for  $\tau$  and  $\beta$  respectively.

#### *Raman Spectrophotometer*

A Delta-Nu Advantage 200A Raman spectrometer was used to determine the structural changes of starch when it is mixed with metal particles. The integration time was 60 seconds using a low resolution and no baseline correction.

#### *Differential Scanning Calorimetry (DSC)*

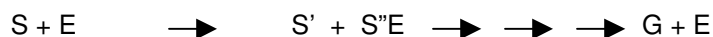
Structural changes attributed to interactions with particles also lead to changes in the thermal transitions observed in starch. These transitions, and their associated heats, can be followed using DSC. A TA Instruments Q20 was used to determine the changes in the enthalpy associated with the presence of interfering interactions. The sampling time was 0.10 seconds/point and the equilibrating temperature was 25°C. The heating ramp temperature was 10-120 °C, followed by an isothermal step maintained for 5 minutes, and a cooling ramp to 25 °C. Indium was used as the calibration standard.

## **Results and Discussion**

### *Enzymatic Degradation*

The single helical structure of amylose in starch can form a complex with charged iodine molecules. Iodine molecules, in the form of I<sub>3</sub><sup>-</sup> ions, enter the coils of solubilized starch chains and the resulting complex gives a blue color to the solution. The iodine atoms form a linear arrangement in the central groove of the helix. Under saturating concentrations of iodine, the color intensity is proportional to the amount of amylose and can be followed using a UV-Vis spectrophotometer. When a solution containing  $\alpha$ -amylase is added, the enzyme attacks the amylose helix and starts digesting it, i.e. cleaves the 1-4 glycosidic bonds, thereby destroying the complex. The decrease in the intensity of the color is expected to be a linear function of the extent of biodegradation. At the completion of digestion no complex remains, and therefore the solution appears transparent in the visible range.

Figure 1 shows the typical UV-Vis spectra as a function of time, of a starch solution containing  $\alpha$ -amylase. Multiple traces are observed because each scan presented was recorded with 2 min interval. A decrease in absorbance around 575 nm is observed as time increases, revealing the time dependent nature of the digestion of starch by the enzyme. A plot of the maximum absorbance at 575 nm versus time will represent the evolution of the following process:



where S, E and G represent starch, the enzyme and glucose respectively, while S' and S'E are cleaved starch molecules that may or may not be still binding to the enzyme. An apparent rate constant  $k$  is associated with the overall process.

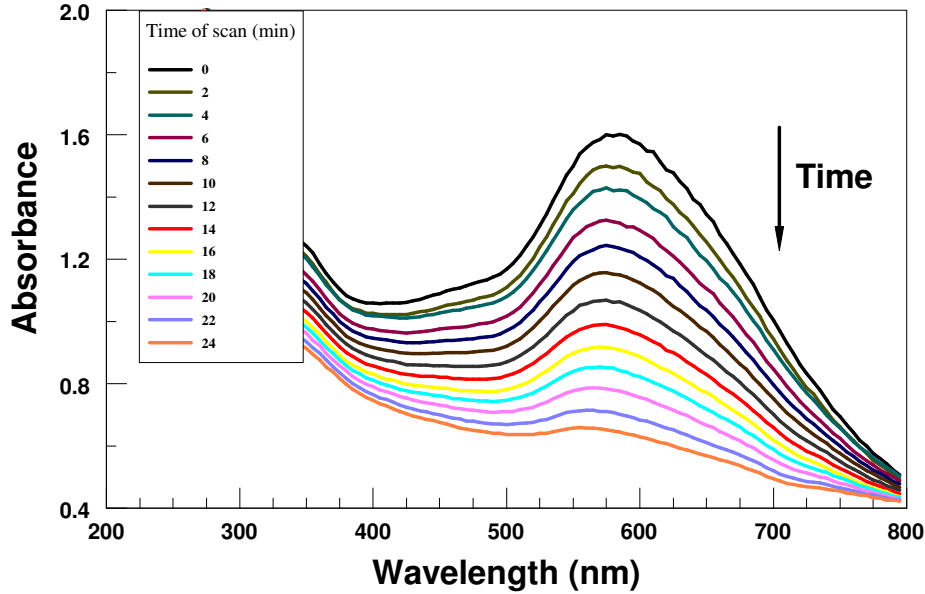


Figure 1 Typical visible spectra of the starch-iodine complex. Each trace represents a scan performed in time increments of 2 minutes.

The digestion kinetics of starch modified by adding two different types of insoluble particles was followed. If the presence of these particles significantly affects the starch structure, the time taken for digestion by the enzyme will vary for each structure. Although in some cases the addition of metal particles directly affects the activity of the enzyme, i.e. reduces or increases its  $k_{cat}/K_M$  value, previous observations indicated that  $TiO_2$  and  $ZnSe$  had no effect on  $\alpha$ -amylase [22]. Therefore, any changes in the rate of digestion, resulting from the addition of these particles, are related to modifications in the starch molecules, which were also demonstrated by Raman spectroscopy and will be discussed later.

#### Modeling of Digestion Kinetics

In order to quantify the enzyme digestion, the absorbance at 575 nm was plotted as a function of time (figure 2). The following equation was used to model the reaction kinetics:

$$Y = e^{-\left(\frac{t}{\tau}\right)^\beta} \quad (1)$$

In this equation,  $Y$  represents the corrected absorbance, i.e. a shift in the absorbance so that the absorbance is 1.0 at  $t = 0$  and 0.0 at  $t = \infty$ .  $t$  represents the actual time in minutes,  $\tau$  represents the characteristic digestion time specific to the process and is the inverse of the apparent rate for the digestion of starch by  $\alpha$ -amylase, and  $\beta$  represents the number of different ways or locations by which the enzyme can attack the amylose molecule (the mechanism of the reaction). The form of this equation, a quasi exponential decay, was chosen because the process analyzed is almost a first order reaction and can be adequately described by an exponential decay function. The “almost” in the above sentence refers to the fact that the mechanism of enzyme attack involves

several points of binding. Note that when  $\beta = 1$ , the order of the process is 1. Also note that the apparent rate constant of the complete process,  $k = 1/\tau$ . The inverse of the rate constant is used throughout this paper because the units of  $\tau$  are in minutes and it's meaning is more intuitively understandable.

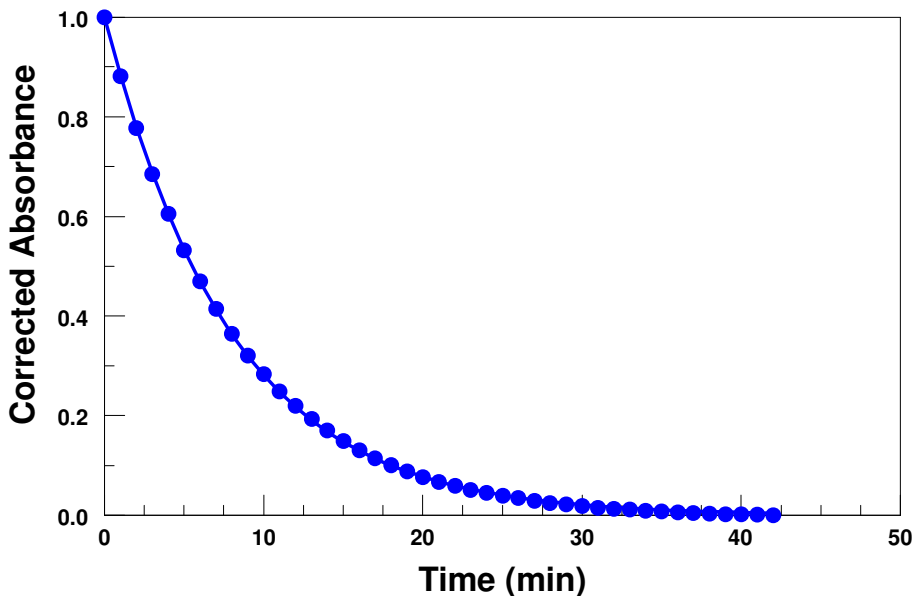


Figure 2 Evolution of the absorbance at 575 nm of iodine-complexed starch during enzymatic digestion. The line represents the fit using equation 1.

#### *Digestion Kinetics of Starch with TiO<sub>2</sub> Particles*

The effect of the presence of TiO<sub>2</sub> particles on the starch structure was first investigated. Two types of particles were used: one in the anatase crystalline form, which has a particle size in the micron range (1-5  $\mu\text{m}$ ), and the other in the rutile form, which has particles in the nanometer size range (10-40 nm). No significant effort was attempted to separate the particles, hence most rutile particles agglomerate into 1  $\mu\text{m}$  sized objects. These anatase and rutile particles were selected to test the effect of crystalline structure and size on the modifications in the structure of starch chains. Since the size of the particles precluded their entrance into the helices, their interaction may be more intermolecular. If this assumption is incorrect, one would expect changes in starch structure and therefore in biodegradation kinetics with the different types of TiO<sub>2</sub>.

Figure 3 shows the evolution of  $\tau$  as a function of increasing amount for both types of particles. As the amount of anatase and rutile particles increases, the time taken to digest the starch chains increases, hence a decrease in the apparent rate constant of the process. Although the presence of these particles clearly affects the digestion rate, figure 3 indicates that there is no significant difference in the times of digestion between the two types of particles. These results suggest that some chemical interactions exist, which affect the chain structure more profoundly.

In an effort to investigate the presence of interactions further, the kinetics of starch biodegradation in the presence of ZnSe was also determined.

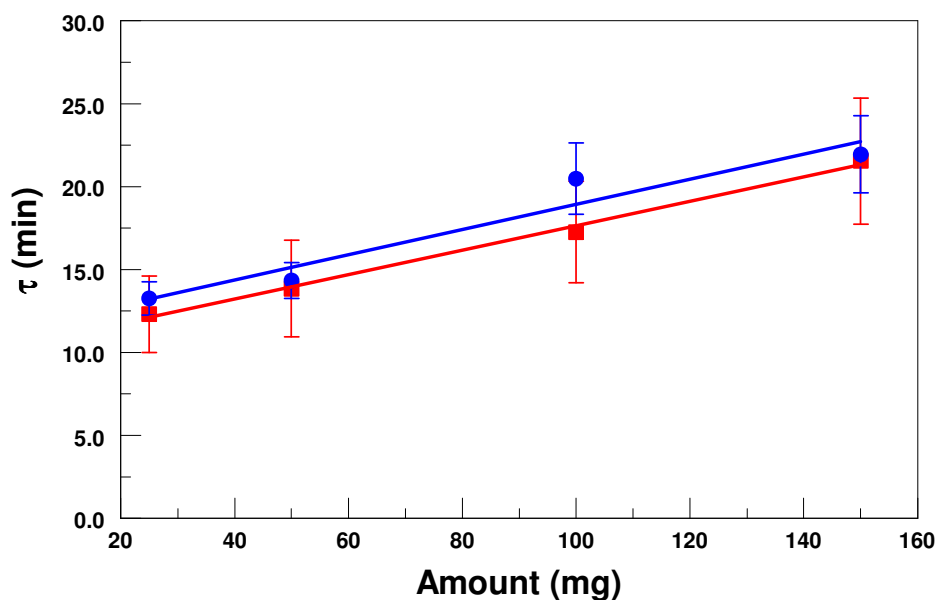


Figure 3 Evolution of the characteristic digestion time ( $\tau$ ) as a function of the amount of anatase and rutile  $\text{TiO}_2$  particles.

#### *Digestion Kinetics of Starch with ZnSe Particles*

Figure 4 shows the evolution of  $\tau$  as a function of the amount of ZnSe particles ( $\sim 5 \mu\text{m}$ ) and demonstrates a clearly distinct behavior from that of  $\text{TiO}_2$ . ZnSe particles have an opposite effect on the time taken for digestion when compared to  $\text{TiO}_2$  i.e. the digestion time decreases as the amount of ZnSe particles increases. Hence, the rate of digestion was increased by the presence of ZnSe particles, which indicates a preferential structure of starch for the enzyme.

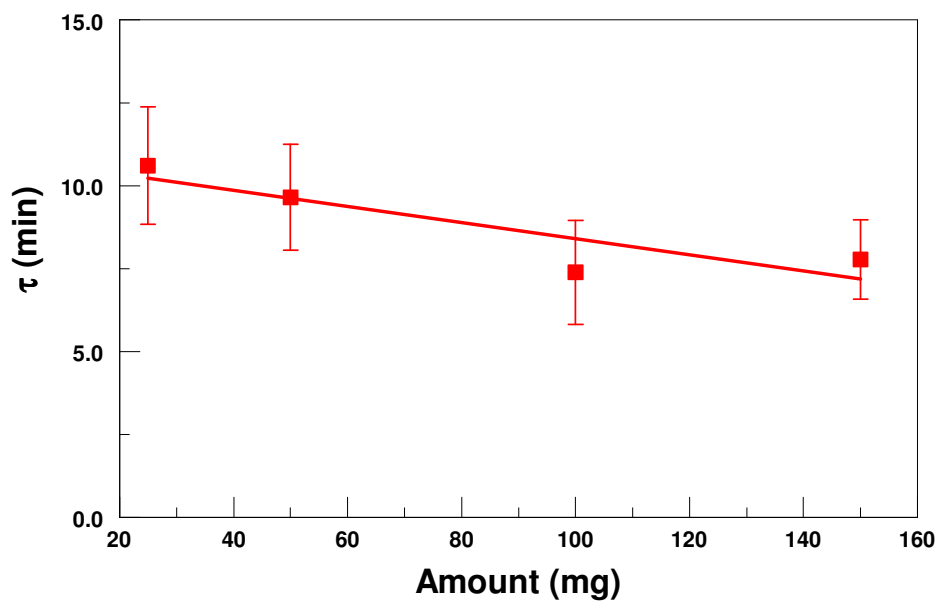


Figure 4 Digestion kinetics of starch with different amounts of ZnSe particles.

Table 1 summarizes all the values of  $\tau$  and  $\beta$  for the biodegradation of starch in the absence and the presence of two types of  $\text{TiO}_2$  particles, anatase and rutile, as well as, ZnSe particles.  $\chi^2$  values represent the accuracy of the fit using equation 1. The values presented above for each sample represents the averages of five samples with the indicated standard deviation. As seen in figures 3 and 4, the  $\tau$  values increase as the amount of  $\text{TiO}_2$  increases and also as the amount of ZnSe decreases. Similar observations are observed for both types of  $\text{TiO}_2$  particles. The standard deviation values show that under the present conditions, the experimental precision is better than the observed changes. The  $\beta$  values for both anatase and rutile particles remain relatively the same compared to pure starch, which suggests that there is no difference in the mechanism of enzyme attack on the substrate. A small decrease is observed in the  $\beta$  values of the starch digestion in the presence of ZnSe particles, which could offer an explanation for the increase in the rate of digestion. However, since the standard deviation is about the same magnitude as the change in  $\beta$ , this may be an experimental artifact. Previous results indicate that the particles do not directly affect the enzyme and therefore the change in characteristic digestion time  $\tau$ , should be attributed to variations in starch chain structure. A more in-depth investigation of the effect of the presence of particles on the starch chain structure is necessary to fully comprehend this system.

Table 1 Fitted parameter values and standard errors for all digestion kinetics experiments.

Type	Concentration (mg/mL)	$\tau$	Stdev	$\beta$	Stdev	$\chi^2$
$\text{TiO}_2$ Rutile	5	13.27	1.01	1.24	0.07	0.0003
	10	14.23	1.08	1.18	0.03	0.0004
	20	20.49	3.42	1.15	0.08	0.0005
	30	21.95	0.33	1.15	0.04	0.0007
$\text{TiO}_2$ Anatase	5	12.32	2.31	1.15	0.08	0.0004
	10	13.85	2.91	1.14	0.16	0.0003
	20	17.26	5.76	1.15	0.08	0.0004
	30	21.55	0.79	1.12	0.06	0.0006
ZnSe	5	10.62	2.02	1.10	0.03	0.0002
	10	9.65	2.22	1.02	0.07	0.0004
	20	7.39	0.62	1.02	0.05	0.0004
	30	7.78	1.20	1.06	0.07	0.0006
Starch		10.78	1.26	1.12	0.12	0.0002

### Differential Scanning Calorimetry Measurements

Figure 5 shows a typical DSC trace of starch dissolved in an aqueous solution. The large endotherm observed is actually composed of three different transitions that not only overlap, but are also interrelated. The large endotherm is quantified by fitting the original trace using three endotherms. The shape of the endotherms was selected to be Gaussian because this shape, although debatable, offered reproducible results and a relative ease in fitting. The software package used to perform this operation was Grams/Al from Thermo-Electron Corporation. For clarity, the resulting endotherms will be named A, B, and C. The transition at the lowest temperature (endotherm A) is associated with disordering of the starch chain, which leads to swelling, as a greater amount of water molecules have access to a larger region of the chain. This swelling in turn causes stresses to occur in certain regions of the starch coil as some entanglements form and tighten. The release of this stress is the cause of the second endotherm (endotherm B), which is observed at higher temperatures. Finally, the motion and pull of the chain caused by the high temperature initiate a disruption of the helices of the starch backbone and a high temperature endotherm (endotherm C) occurs, usually above the boiling temperature of water. Because of this, all traces were recorded using hermetic aluminum sample pans.

Figures 6 and 7 show the DSC traces of solubilized starch in the presence of different amounts of  $\text{TiO}_2$  in the anatase structure. In both the original and fitted traces of figures 6 and 7 the major difference observed is the clear change in the relative amount of the third endotherm at high temperature. As the concentration of  $\text{TiO}_2$  increases, the heat associated with this endotherm increases. A more quantitative analysis was attempted using the peaks fitted to the traces.

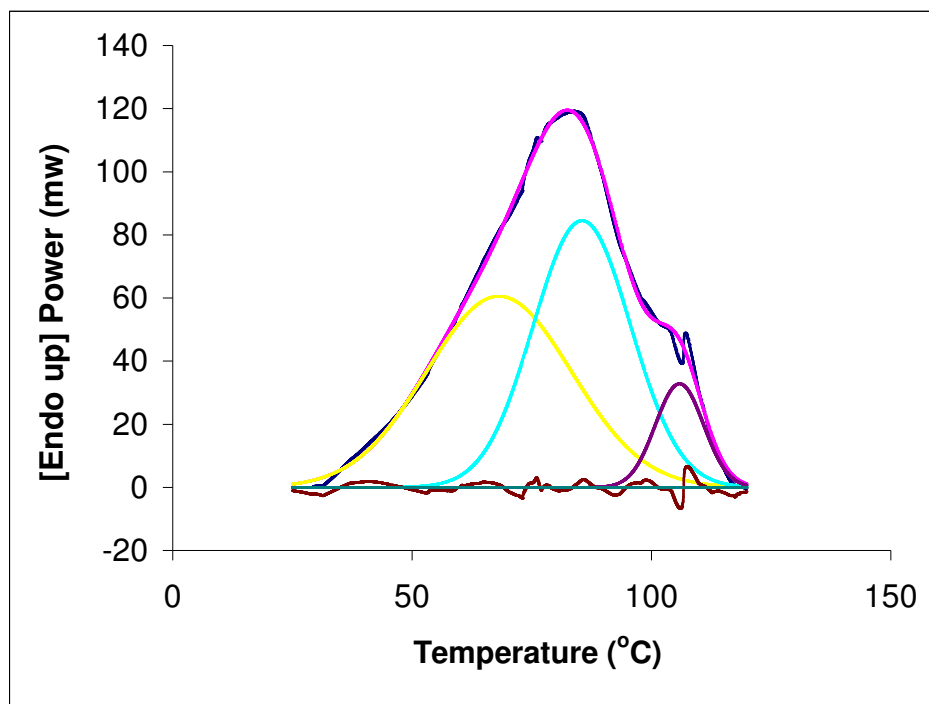


Figure 5 Typical DSC trace of starch (25% in  $\text{H}_2\text{O}$  W/W). The original endotherm is a combination of three endotherms that overlap. Simulation software was used to isolate these underlying endotherms. See text for details.

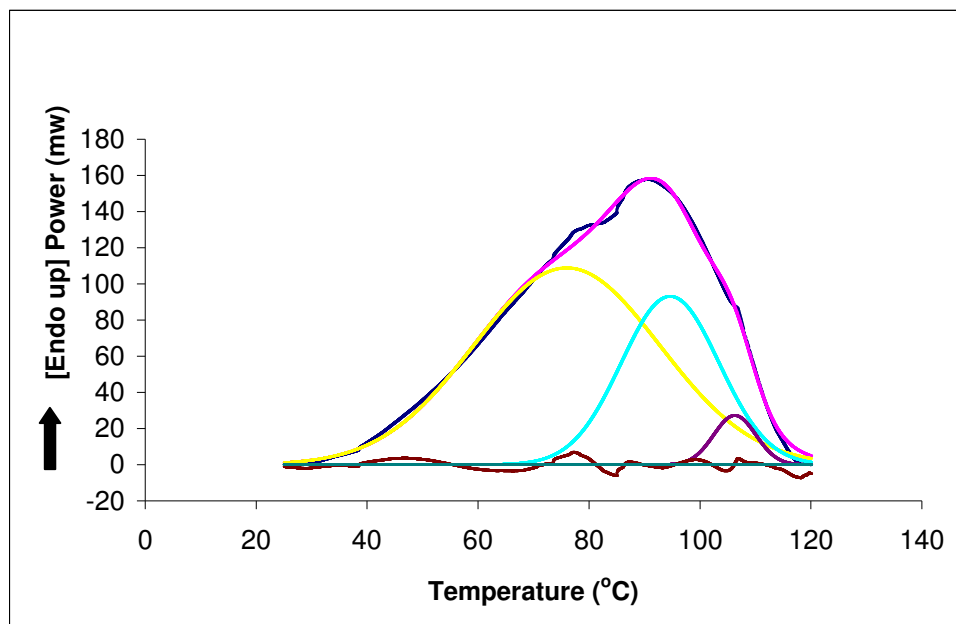


Figure 6 DSC curve for starch (25% in H<sub>2</sub>O W/W) with 25 mg of TiO<sub>2</sub> (anatase) particles. The original endotherm is a combination of three endotherms that overlap. Simulation software was used to isolate these underlying endotherms. See text for details.

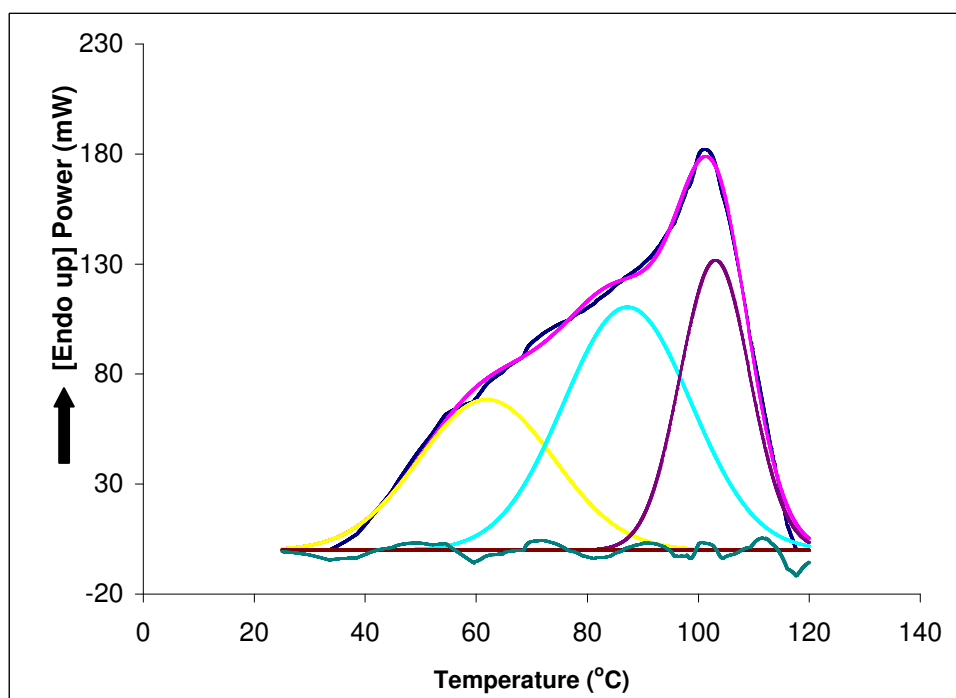


Figure 7 DSC curve for starch (25% in H<sub>2</sub>O W/W) with 150 mg of TiO<sub>2</sub> (anatase) particles. The original endotherm is a combination of three endotherms that overlap. Simulation software was used to isolate these underlying endotherms. See text for details.

Table 2 shows the average fraction of each endotherm and their standard deviations under various conditions. The data shows a small but significant decrease in the fraction of endotherm A, for both forms of TiO<sub>2</sub>, as the amount of particles is increased. The fraction of endotherm B, however, is relatively constant under the same conditions, while a large increase in the fraction of endotherm C is observed. In the case of increasing the amount of ZnSe particles, the data shows that the fraction of endotherm A is relatively constant but the fraction of endotherm B decreases, suggesting a lower amount of stress in the starch chains which could account for the observed increase in rate of degradation. However, the fraction of endotherm C increases for ZnSe as for TiO<sub>2</sub> with increasing amounts of particles. These results suggest that the particles affect the structure of the starch chains resulting in a disruption of transitions A, B, and C. The DSC traces do not indicate the nature of the structural changes. Hence, Raman spectroscopy was used to further probe the molecular nature of the interactions between starch and particles.

Table 2 Summary of the relative fractions of the endotherms observed in DSC.

Type	Concentration (mg/mL)	Peak A		Peak B		Peak C	
		Fractions (Area)	Stdev	Fractions (Area)	Stdev	Fractions (Area)	Stdev
TiO <sub>2</sub> Rutile	5	0.56	0.13	0.38	0.12	0.06	0.01
	10	0.72	0.17	0.22	0.14	0.06	0.07
	20	0.51	0.19	0.37	0.24	0.12	0.08
	30	0.32	0.10	0.40	0.05	0.28	0.02
TiO <sub>2</sub> Anatase	5	0.62	0.07	0.32	0.03	0.06	0.03
	10	0.59	0.16	0.33	0.11	0.08	0.07
	20	0.21	0.04	0.38	0.18	0.41	0.19
	30	0.51	0.08	0.35	0.10	0.14	0.02
ZnSe	5	0.33	0.21	0.62	0.23	0.05	0.02
	10	0.46	0.13	0.45	0.20	0.09	0.01
	20	0.28	0.03	0.06	0.02	0.66	0.01
	30	0.32	0.19	0.40	0.07	0.28	0.14
Starch		0.38	0.13	0.51	0.10	0.11	0.03

### Raman Spectroscopy Analysis

#### Starch Aqueous Solution

Figure 8 shows a typical Raman spectrum of an aqueous solution of pure starch (dark blue continuous line) and starch with two types of particles (discussed later). Only the region between 400 and 1500 cm<sup>-1</sup> is presented. Several bands are observed. The Raman band at 450 cm<sup>-1</sup> in figure 8 was attributed to the skeletal modes of the pyrose ring; the band at 734 cm<sup>-1</sup> was attributed to the stretching of the C-C bond, while the band at 865 cm<sup>-1</sup> was attributed to the deformation vibrations of C-H and CH<sub>2</sub>. One of the most important bands in this study is found around 934 cm<sup>-1</sup> and is attributed to the skeletal mode vibrations of  $\alpha$ -1, 4 glycosidic bond (C-O-C). Other bands of significant interest occur at 1087 cm<sup>-1</sup> due to C-O-H bending vibrations, at 1122 cm<sup>-1</sup>, attributed to C-O stretching and C-O-H bending vibrations. A group of bands around 1260-1280 cm<sup>-1</sup> are related to CH<sub>2</sub>OH, side chains modes of vibrations. A large band located around 1339 cm<sup>-1</sup> is attributed to C-O-H bending and CH<sub>2</sub> twisting vibrations.

## Starch Aqueous Solutions in the Presence of Particles

No significant changes in the intensity of the Raman bands are observed as a function of the amount of either type of particles. However, some peaks shifts occur relative to pure starch. Figure 8 compares the Raman spectra of starch, starch with TiO<sub>2</sub>-anatase, and starch with ZnSe particles using similar amounts (100 mg). A clear shift is observed in the position of the peaks below 1500 cm<sup>-1</sup> that are assigned to glycosidic and backbone vibrations. The presence of TiO<sub>2</sub> particles shifts the bands to higher wavenumbers indicating more rigid bonds while the addition of ZnSe shifts the same bands to lower wavenumbers implying that the interaction with ZnSe weakens the covalent bonds of the disrupted groups. This indicates that the starch chain containing or interacting with ZnSe will be more flexible resulting in less stress and more easily deformable helices. In addition, the increased flexibility may be the cause of the increase in biodegradation rate as the enzyme may bind to the side of the chains with less hindrance.

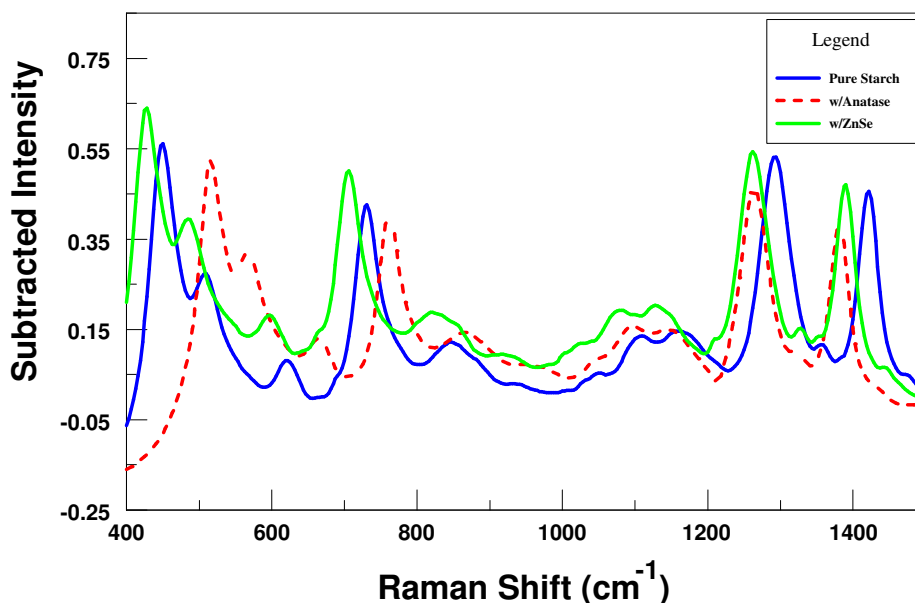


Figure 8 Comparison of the Raman spectra of starch, starch with TiO<sub>2</sub> (anatase), and starch with ZnSe particles. The spectra have been background corrected and normalized for comparison.

The implication of an increase or decrease in stress on the backbone chain depending on the nature of the particles leads us to suggest that the particles interact chemically with the starch molecules by increasing or decreasing the strength of the intramolecular bonds. Hence, we propose that the backbone structure of starch is modified through interactions with particles. These interactions vary the stress and flexibility of the backbone, which could explain all the kinetic, thermal and spectroscopy observations.

The increase in digestion time as well as the increase in the spring constants associated with the backbone vibrations of starch in the presence of TiO<sub>2</sub>, suggest that the TiO<sub>2</sub> particles form stress-increasing interactions. The decrease in digestion time, the decrease in the spring constants associated with the backbone vibrations of starch as well as the greater fraction of endotherm C in the presence of ZnSe compared to TiO<sub>2</sub>, suggest that the ZnSe particles form stress decreasing interactions.

## Conclusions

This paper reports the investigation of the variations of the kinetics of enzymatic cleavage of modified starch, obtained by mixing starch with various types of particles. The rates of biodegradation were investigated by fitting the cleaving process to a quasi-exponential decay equation, from which values of  $\tau$  and  $\beta$  were determined. Four types of samples were investigated: starch alone, and in the presence of TiO<sub>2</sub> (anatase), TiO<sub>2</sub> (rutile) and ZnSe particles. Results show that the rate of biodegradation is decreased in the presence of any form of TiO<sub>2</sub>, while it is increased when starch is mixed with ZnSe.

DSC traces were also recorded for the four types of samples. Three endothermic transitions were observed that correspond to: A, the disordering of the starch coils, B, the relaxation of the stressed physical entanglements, and C, the disordering of the helices. Significant changes in the amount of the later endotherm (C), with different types and amounts of particles were found. These changes were correlated with Raman studies of the different types of samples. Significant shifts occurred in the presence of TiO<sub>2</sub> (to higher vibrational energies) and ZnSe (to lower vibrational energies). These results suggest that the effect of the presence of ZnSe on the structure of starch chains is that chain interactions with ZnSe weaken the covalent bonds of the disrupted groups resulting in more flexible chains that have less stressed and more easily deformable helices. The increased flexibility is believed to be the cause of the increased rate of the biodegradation process, as the enzyme may bind to the side of the chains with less hindrance.

## Acknowledgments

Partial funding was gratefully provided by grants from the Texas Higher Education Coordinating Board, Advanced Research Program (ARP – Grant No. 003581-0001-2006) and from the Welch Research Foundation (V-004).

## References

1. Roesser, D. S.; McCarthy, S.P.; Gross, R. A. *Macromolecules* 1996, 29, 1-9.
2. Kizil, R.; Irudayaraj, J.; Seetharaman, K. *J. Agri. Food Chem.* 2002, 50, 3912-3918.
3. Weurding, R. E.; Enting, H; Verstegen, M. W. A; *Poultry Science* 2003, 82, 279-284.
4. Tester, R. F.; Karkalas, J.; Qi, X. *World's Poultry Science Journal* 2004, 60, 186-195.
5. Liu, Y.; Himmelsbach, D.S.; Barton, F. E. *Applied Spectroscopy* 2004, 58, 745-749.
6. Galliard, T; Ed. "Starch Properties and Potential", Wiley, NY, 1987.
7. French, A. D; "Starch: Chemistry and Technology", Academic Press, NY, 2<sup>nd</sup> Ed. 1984.
8. Rappenecker, G; Zugenmaier, P; *Carbohydr. Res.* 1981, 89, 11-19.
9. Murphy, V. G; Zaslow, B; French, A. D; *Biopolymers*, 1975, 14, 1487-1501.
10. Gessler, K; Uson, I; Takaha, T; Krauss, N; Smith, S. M; Okada, S; Sheldrick, G. M; Saenger, W; *Proc. Natl. Acad. Sci.* 1999, 96, 4246-4251.
11. Alias, J.; Goni, I.; Gurruchaga, M. *Polym. Degradation and Stability* 2007, 92, 658-666.
12. Rao, P. S. Studies on the nature of carbohydrate moiety in high yielding varieties of rice. *J. Nutr.* 1971, 101, 879-884.

13. You, S.; Izydorczyk, M. S. *Carbohydrate Polymers* 2007, 69, 489-502.
14. Zhang, G.; Ao, Z.; Hamaker, B. R. *Biomacromolecules* 2006, 7, 3252-3258.
15. Benmoussa, M.; Moldenhauer, K. A. K.; Hamaker, B. R. *J. Agric. Food. Chem.* 2007, 55, 1475-1479.
16. Zhang, G.; Venkatachalam, M.; Hamaker, B. R. *Biomacromolecules* 2006, 7, 3259-3266.
17. Mulhbachher, J.; Mateescu, M. A. *International Journal of Pharmaceutics* 2005, 297, 22-29.
18. Dumoulin, Y.; Alex, S.; Szabo, P.; Carilier, L.; Mateescu, M.A.; *Carbohydrate Polymers* 1998, 37, 361-370.
19. Jane, J; *J. Macromol Sci; Pure & Appl. Chem.* 1995, A32, 751-757.
20. Lewen, K. S; Paeschke, T.; Reid, J.; Molitor, P.; Schmidt, S. J. *J. Agri. Food Chem.* 2003, 51, 2348-2358.
21. Sanchez, R. F; Bernazzani, P; "Evolution of the Glass Transition Temperature of Polystyrene with Different Particle-Surface Interactions" Poster presentation at the International Polyolefins Conference, Houston, Texas, USA, February 2008.
22. Unpublished results, 2007.